

# Improved Leakage Current for TiO<sub>2</sub>-Based MIM Capacitors by Embedding Ge Nanocrystals

Yu-Hsun Chen, Meng-Ting Yu, Chia-Chun Lin, and Yung-Hsien Wu\*

Department of Engineering and System Science, National Tsing Hua University, 300, Hsinchu, Taiwan

Phone: +886-3-516-2248 Email: [yunhwu@mx.nthu.edu.tw](mailto:yunhwu@mx.nthu.edu.tw)

## I. Introduction

Metal-insulator-metal (MIM) based capacitors have been recently perceived as feasible passive components for radio frequency (RF), analog and mixed signal integrated circuits. With the advent of high-permittivity (high- $\kappa$ ) dielectric, the requirement of large area to implement high-capacitance capacitors is relieved. The booming field of high- $\kappa$  dielectric development has ushered in a new era for high-performance MIM capacitors. Among various kinds of high- $\kappa$  dielectrics, TiO<sub>2</sub> has long attracted great attention because its  $\kappa$  value can be as high as 90~170 when it crystallizes in rutile phase, depending on the lattice orientation. Even with the potential to achieve a high  $\kappa$  value, one inherent material property that limits TiO<sub>2</sub> from further application in MIM capacitors is its high electron affinity which consequently results in high leakage current. Therefore high-work function electrode is always employed for TiO<sub>2</sub>-based MIM capacitors to suppress leakage current. In addition, many efforts have been made on doping of TiO<sub>2</sub> with specific metal element to improve its leakage performance such as TiO<sub>2</sub>-LaAlO [1], TiTaO [2], TiNiO [3], TiHfO [4], TiZrO [5], and TiPrO [6]. Although doped TiO<sub>2</sub> demonstrates promising results, maintaining the dopant uniformity requires rigorous process control. In fact, reduced leakage can also be obtained by stacking another dielectric with larger band gap such as SiO<sub>2</sub>/TiO<sub>2</sub> stack [7]. However, the capacitance density will be inevitably compromised because a larger band gap dielectric usually accompanies a lower  $\kappa$  value. Different from prior arts, in this work, significantly improved leakage current performance for TiO<sub>2</sub>-based MIM capacitors can be accomplished by introducing Ge nanocrystals (NCs) into TiO<sub>2</sub>. Embedding NCs in dielectrics have been widely adopted in the technology of charge trap flash memory because additional trapping sites can be provided to store injected electrons. Nevertheless the function of charge storage is not required for MIM capacitors, the main reason to introduce NCs is to induce the so-called Coulomb blockade effect or build an internal field to compensate the applied external one, and therefore reduced leakage current can be expected. The results in this work prove the idea by demonstrating a relatively high capacitance density of 25.2 fF/ $\mu\text{m}^2$  with leakage current of  $4.6 \times 10^{-7}$  A/cm<sup>2</sup> at -1 V, which is lower than capacitors without incorporating Ge NCs by a factor of ~1000. In addition, the Ge NCs embedded MIM capacitors show a small loss tangent of 0.020, a low temperature coefficient of capacitance (TCC) of 88 ppm/ $^{\circ}\text{C}$ . These promising electrical characteristics attest to the eligibility of the novel structure for MIM applications.

## II. Experiment

50-nm Pd was deposited on SiO<sub>2</sub>/Si as the bottom electrode of MIM capacitors. Then 29-nm TiO<sub>2</sub> film was deposited as the dielectric of capacitors (denoted as TiO<sub>2</sub> sample). Subsequently, rapid thermal annealing (RTA) of 500  $^{\circ}\text{C}$  was performed to crystallize TiO<sub>2</sub>. To explore the impact of Ge NCs incorporation on electrical characteristics, aforementioned 29-nm TiO<sub>2</sub> was replaced with TiO<sub>2</sub>/Ge/TiO<sub>2</sub> laminate structure of 12.5/1.5/12.5 nm for some samples (denoted as TiO<sub>2</sub>-Ge sample). With the same RTA condition, Ge NCs embedded in the crystalline TiO<sub>2</sub> is also formed. Next, nitrogen plasma treatment (NPT) was performed on some samples to investigate how nitrogen

radicals affect device performance. Finally 50-nm Pd was formed as the top electrode. Brief process flow and device structure are shown in Fig. 1.

## III. Results and Discussion

Fig. 2 shows the capacitance-voltage (C-V) curves for different process conditions. At 0 V, TiO<sub>2</sub> samples display the highest capacitance density of 33.8 fF/ $\mu\text{m}^2$  while the value for TiO<sub>2</sub>-NPT and TiO<sub>2</sub>-Ge-NPT samples decrease to 30.2 fF/ $\mu\text{m}^2$  and 25.2 fF/ $\mu\text{m}^2$  respectively. Apparently, NPT process significantly mitigates the dependence of capacitance on applied voltage which makes the capacitors more feasible in circuit applications. As shown in Fig. 3, the  $\kappa$  value of TiO<sub>2</sub> is 110.8 which implies the formation of crystalline dielectric after RTA. With NPT treatment, the  $\kappa$  value slightly decreases to 99.0 which is due to the formation of TiON [7]. With additional incorporation of Ge NCs, the  $\kappa$  value further drops to 75.5 because Ge has a much smaller  $\kappa$  value than TiO<sub>2</sub>. Although additional plasma treatment or incorporation of Ge NCs results in capacitance degradation, it gains much improved leakage current performance as evidenced in Fig. 4. Because nitrogen radicals well passivate grain-boundary-related defects in the crystalline TiO<sub>2</sub> film, at bias voltage of -1 V, TiO<sub>2</sub>-NPT samples demonstrates reduced leakage current by a factor of 3125 as compared to TiO<sub>2</sub>-samples. For TiO<sub>2</sub>-Ge-NPT samples, the leakage current further reduces to  $4.6 \times 10^{-7}$  A/cm<sup>2</sup> at -1 V, nearly 3 orders lower than TiO<sub>2</sub>-NPT samples. Note that from separate experiments, among these 3 process conditions, TiO<sub>2</sub>-Ge-NPT samples enjoy the lowest leakage current under the same capacitance density (not shown). The mechanism of NCs induced leakage current improvement can be understood by the band diagram shown in Fig. 5. Due to the conduction band offset of 0.33 eV between Ge NCs and rutile TiO<sub>2</sub> [8], part of the injected electrons from the electrode would be trapped in the Ge NCs. Once NCs are filled with electrons, it may prevent subsequent electrons from further injection by Coulomb blockade effect or build an internal electric field that suppresses subsequent electron injection by compensating the external electric field, and therefore reduced leakage current is expected. Fig. 6 shows the dependence of normalized capacitance on measurement temperature. For samples with NPT, Ge incorporation indeed helps improve TCC from 113 to 88 ppm/ $^{\circ}\text{C}$ . The phenomenon can be explained by the reduced electron injection which causes higher relaxation time and consequently leads to a smaller capacitance variation. Besides the requirement of low leakage current and small TCC, low dielectric loss is also a prerequisite for passive element applications. Dielectric loss quantifies the inherent electrical energy dissipation of a dielectric and the results are shown in Fig. 7. At 1 MHz, loss tangent for TiO<sub>2</sub>-NPT samples is about 0.045 and the value becomes 0.020 for TiO<sub>2</sub>-Ge-NPT samples, which is improved by a factor of 2.2. Since loss tangent is dependent on conductance of the dielectric, once the leakage current can be reduced, improved loss tangent is expected as TiO<sub>2</sub>-Ge-NPT samples. Table I summarizes the major device parameters for TiO<sub>2</sub>-based [3, 4, 7, 9] and other recent [10] MIM capacitors with various electrodes. It is confirmed that plasma treatment of Ge NCs-embedded TiO<sub>2</sub> provides another promising avenue to obtain high capacitance density with much improved leakage current.

#### IV. Conclusion

Nitrogen plasma treatment was proven as an efficient approach to reduce leakage current of crystalline TiO<sub>2</sub> because of passivation of grain boundary related defects. Further improved leakage performance can be achieved by incorporating Ge NCs into TiO<sub>2</sub>. MIM capacitors formed by integrating these processes hold the great potential for future applications in terms of high capacitance density of 25.2 fF/μm<sup>2</sup> with a large value of 75.5, low leakage current of 4.6×10<sup>-7</sup> A/cm<sup>2</sup> at -1 V, small TCC of 88 ppm/°C and desirable loss tangent of 0.020.

#### Acknowledgement

This work was supported by the National Science Council of Taiwan under Contract NSC 101-2628-E-007-012-MY3 and NSC 101-2120-M-009-004.

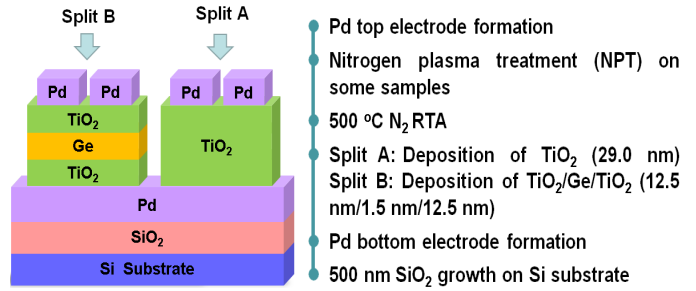


Fig. 1 Process flow of TiO<sub>2</sub>-based MIM capacitors. The device structure is not to scale.

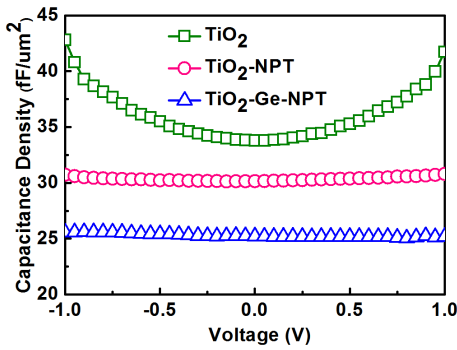


Fig. 2 C-V characteristics for different TiO<sub>2</sub>-based dielectrics measured at 1 MHz. Significant dependence of capacitance on voltage can be alleviated by plasma treatment.

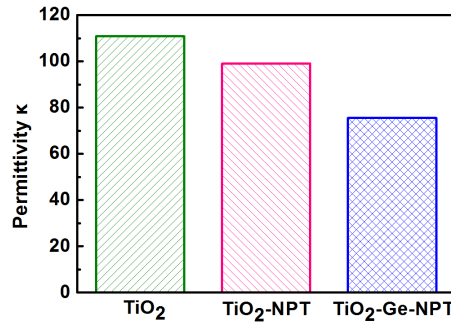


Fig. 3 κ value for different TiO<sub>2</sub>-based dielectrics extracted from zero-biased capacitance. The κ value higher than 100 for TiO<sub>2</sub> suggests the crystalline structure.

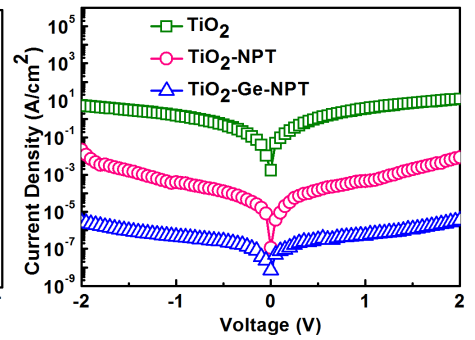


Fig. 4 I-V characteristics for different TiO<sub>2</sub>-based dielectrics at room temperature. TiO<sub>2</sub>-Ge-NPT shows the lowest leakage under the same capacitance (not shown).

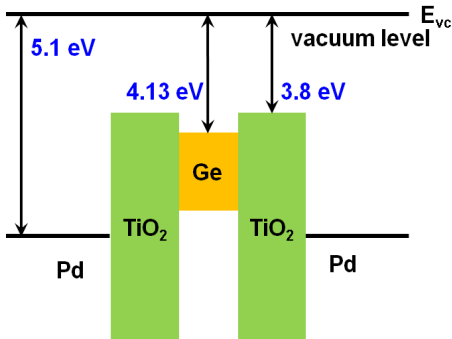


Fig. 5 Band diagram (not to scale) for TiO<sub>2</sub>/Ge/TiO<sub>2</sub> MIM capacitors with Pd as electrodes.

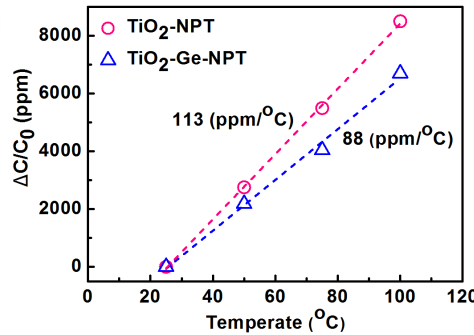


Fig. 6 Temperature-dependent normalized capacitance for TiO<sub>2</sub> dielectric with and without Ge NCs incorporation.

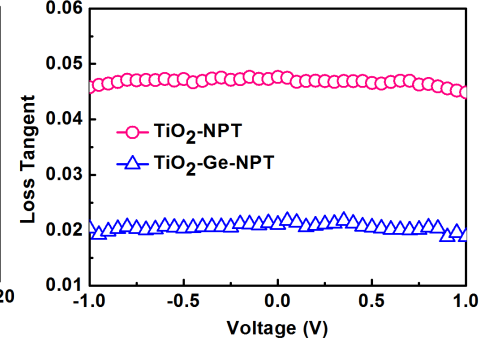


Fig. 7 Loss tangent for TiO<sub>2</sub> dielectric with and without Ge NCs incorporation measured at 1 MHz.

Table I Comparison of major device parameters of TiO<sub>2</sub>-based and other recent MIM capacitors with various electrodes.

Material	TiNiO [3]	TiHfO [4]	TiO <sub>2</sub> /SiO <sub>2</sub> [7]	TiO <sub>2</sub> [9]	Gd <sub>2</sub> O <sub>3</sub> /Eu <sub>2</sub> O <sub>3</sub> [10]	TiO <sub>2</sub> /Ge/TiO <sub>2</sub> This work
Thickness (nm)	20	12	14/2.5	25	8/8	12.5/1.5/12.5
Top/Bottom Electrode	Ni/TaN	TaN/TaN	Al/TaN	Ni <sub>2</sub> Si/Ni <sub>2</sub> Si	Pt/Pt	Pd/Pd
Work function (eV)	5.1/4.6	4.6/4.6	4.3/4.6	4.8/4.8	5.6/5.6	5.1/5.1
Capacitance Density (fF/μm <sup>2</sup> )	17.1	28	11.9	17	12.5	25.2
Current Density at -1 V (A/cm <sup>2</sup> )	7.7 × 10 <sup>-6</sup>	4.8 × 10 <sup>-6</sup>	8.3 × 10 <sup>-7</sup>	6.4 × 10 <sup>-6</sup>	1.2 × 10 <sup>-5</sup>	4.6 × 10 <sup>-7</sup>

#### References

- [1] C. H. Cheng et al., JES, **157**, H821, 2010.
- [2] K. C. Chiang et al., Symp. VLSI Tech., 2005, 62.
- [3] C. C. Huang et al., ECS Lett., **10**, H287, 2007.
- [4] C. H. Cheng et al., TED, **29**, 1105, 2008.
- [5] C. H. Cheng et al., JES, **155**, G295, 2008.
- [6] C. Huang et al., JES, **156**, G23, 2009.
- [7] Y. H. Wu et al., EDL, **33**, 104, 2012.
- [8] D. Tsukamoto et al., ACS Catal., **2**, 599, 2012.
- [9] J. H. Lee et al., TED, **58**, 672, 2011.
- [10] R. Padmanabhan et al., TED, **60**, 1523, 2013.